Study of Impedance and Radiation Properties of a Concentric Microstrip Triangular-Ring Antenna and Its Modeling Techniques Using FDTD Method

Iti Saha Misra and S. K. Chowdhury, *Senior Member, IEEE*

***Abstract*— A concentric microstrip triangular-ring antenna structure using the log-periodic principle for increasing the impedance bandwidth of the microstrip patch antenna is described. The finite-difference time-domain (FDTD) method is applied to analyze the proposed structure. A special technique to model the slanted metallic boundaries of the triangular ring has been used in the general FDTD algorithm to avoid the staircase approximation. The method improves the accuracy of the original FDTD algorithm without increasing the complexity. The radiation patterns at different frequencies over wide-band width are obtained experimentally.**

***Index Terms*—FDTD methods, microstrip antennas.**

I. Introduction

A three-element concentric microstrip triangular-ring antenna (CMTRA) has been designed using a log-periodic principle and fabricated on a polytetra fluroethylene (PTFE) substrate. The elements of the CMTRA are fed electromagnetically by a 50-Ω microstrip line. The impedance and radiation characteristics have been measured and compared with those of two single triangular-ring antennas (STRA) having the largest and the smallest element dimensions of the CMTRA. The impedance variation for the CMTRA has been measured at different feed locations. Results show that the bandwidth of the CMTRA is increased with respect to the STRA and the maximum bandwidth obtained for a particular feed location away from the center. The measured radiation characteristics at different feed location show its invariant nature. The measured impedance pattern for two feed locations are verified by FDTD method. This method is similar to the method described for concentric microstrip circular-ring antenna (CMCRA) in [1]. A special technique to model the slanted metallic boundaries of the triangular ring has been used in the general FDTD algorithm to avoid the staircase approximation [2], [3]. The method improves the accuracy of the original FDTD algorithm without increasing the complexity.

II. Design of Three-Element CMTRA

The three-element CMTRA is shown in Fig. 1(a). The width "w" and spacing "d" between the elements are specified in this figure. First, the innermost element was chosen with side $a = 1.4$ cm and width $w = 0.2$ cm. The spacing between the adjacent elements and their widths are then chosen maintaining the following relation:

$$\tau = d_{n+1}/d_n = w_{n+1}/w_n = 1.25 \tag{1}$$

where n is the suffix of the nth number of patch as indicated in Fig. 1(a). The ring width and spacing decrease from the innermost element to the outermost element. Maintaining this relation the outermost ring has the sides $a = 3.0$ cm and width $w = 0.128$ cm. The STRA's investigated have the smallest

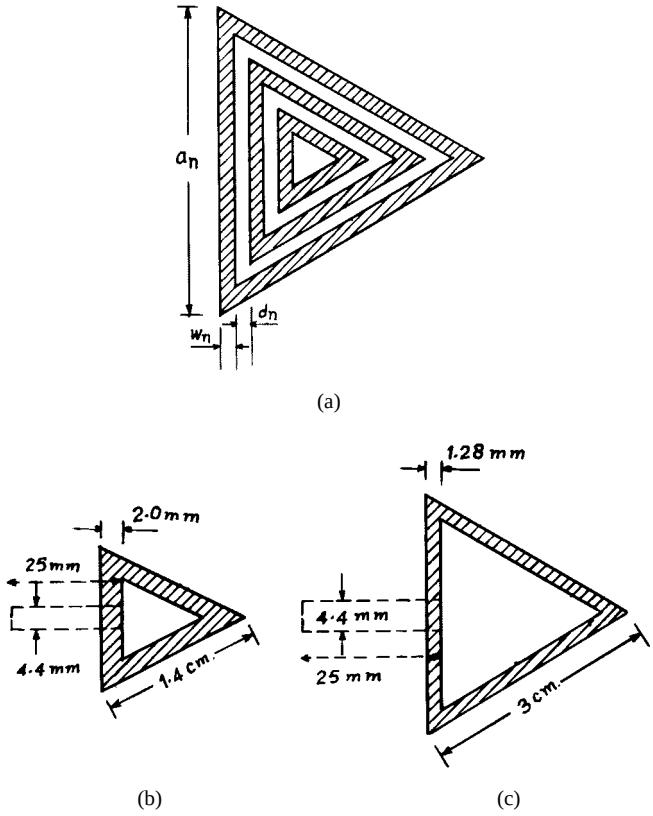

Fig. 1. Geometry of (a) three-element CMTRA, (b) STRA investigation of the smallest element dimensions, and (c) STRA investigation of the largest element dimensions.

Manuscript received September 6, 1996; revised May 30, 1997.

The authors are with the Department of Electronics and Telecommunication Engineering, Jadavpur University, Calcutta, 700 032 India.

Publisher Item Identifier S 0018-926X(98)02680-5.

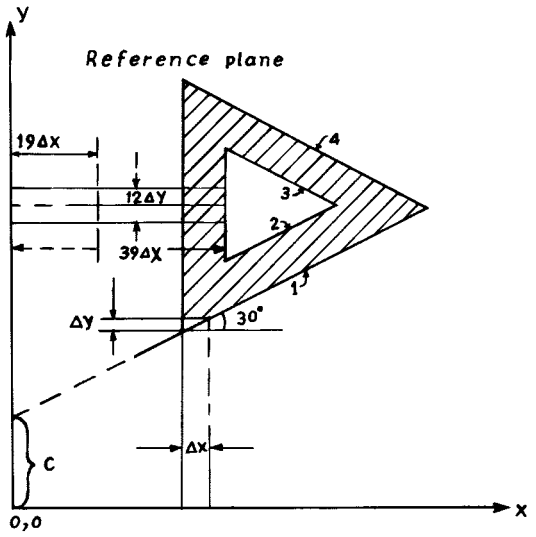

Fig. 2. Modeling of triangular ring in FDTD domain.

and the largest element dimensions of the CMTRA as given in Fig. 1(b) and (c), respectively.

III. Analysis of CMTRA and Single Triangular Ring by FDTD Method

In this investigation one CMTRA and two triangular rings having the largest and smallest element dimensions of the CMTRA are analyzed by FDTD method. These antennas are fed electromagnetically by a 50-Ω microstrip line which was fabricated on PTFE substrate with dielectric constant 2.55 and thickness 0.159 cm (Fig. 1). The application of FDTD method to these antennas are similar to those of CMCRA [1]. However, the modeling of the triangular-ring element is different. In the following sections, we will describe the modeling techniques of triangular ring in the FDTD domain.

A. Modeling of Larger Triangular Ring

Fig. 2 shows the actual dimension of the triangular ring antenna in the X-Y plane of the FDTD domain. Since the ring is an equilateral triangle the angle between the X axis and slanting plane is 30°. All the slanting sides of this ring can be represented by the equation of a line as

$$y = mx + C \cdots \tag{2}$$

where $m = \tan\theta$, $\theta =$ angle between the X axis and slanting plane.

Putting the value of θ and any coordinate (x, y) passing through the line, the value of C can be found out.

Now, if one can select the proper aspect ratio of each cell in the FDTD domain, then the slanted plane wall can be modeled exactly, i.e., it is possible to locate the boundary nodes of the mesh exactly on the slanted planes [3]. In this particular case if we select $\Delta x = 0.64$ mm and, hence, $y = \Delta x \tan\theta$ then for every space increment along X and Y direction the equation of the line will be well maintained.

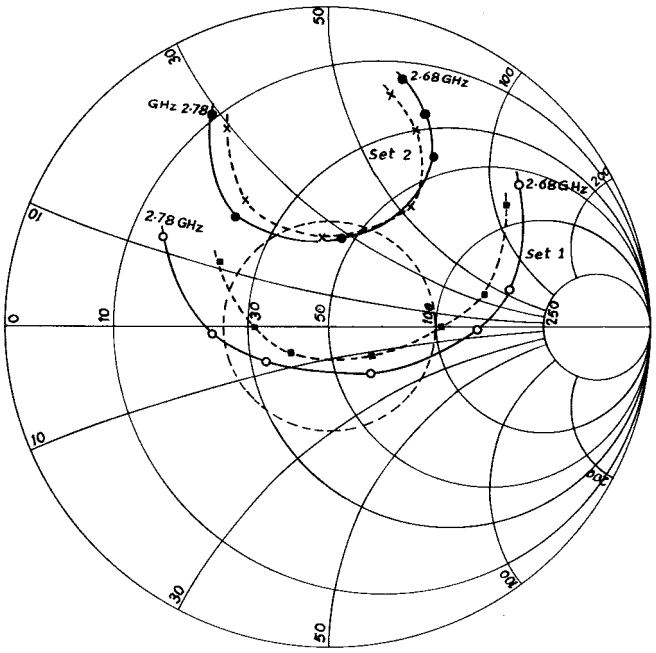

Fig. 3. Impedance plot of largest triangular ring of Fig. 1(c) at different feed location—set 1 for center feed, set 2 for 0.35 cm off-center feed.

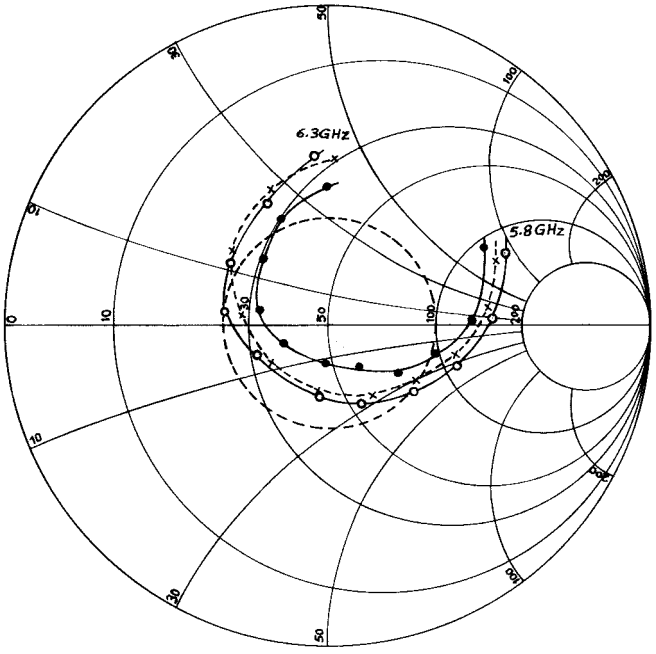

Fig. 4. Impedance plot of smallest triangular ring of Fig. 1(b) for center feed.

The tangential electric field components E_x and E_y and normal component of magnetic field H_z were made equal to zero on the triangular-ring patch bounded by the six lines. The FDTD parameters for this ring were: $\Delta x = 0.64$ mm, $\Delta y = 0.57735\Delta x = 0.3694$ mm, and $\Delta z = 0.5926$ mm, $\Delta t = \Delta y/2C_0$ ($C_0 =$ free-space velocity of light), and Guassian half-width $\tau = 18$ ps. The distance between the source plane to microstrip antenna was $39\Delta x$ and the reference plane was set at a distance $19\Delta x$ from the source plane. The

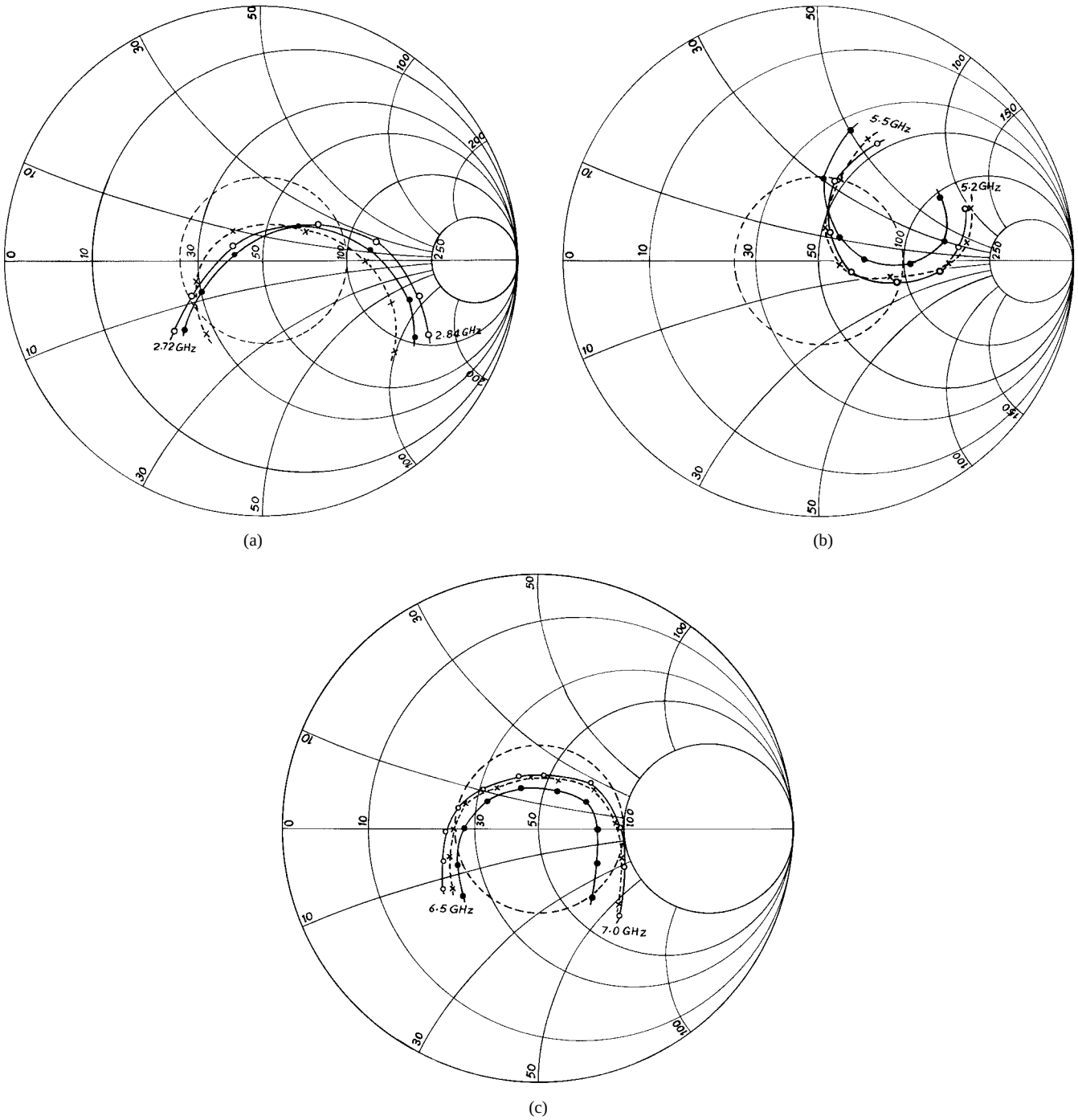

(a) (b) (c)

Fig. 5. (a) and (b) Impedance plot of three-element CMTRA at different frequency band for center feed. (c) Impedance plot of three-element CMTRA at different frequency band for center feed.

50-Ω microstrip line width and the ring width were modeled as $12\Delta y$ and $2\Delta x$, respectively.

B. Modeling of Small Triangular Ring

The actual dimensions of the small triangular ring is shown in Fig. 1(b). The FDTD parameters were $\Delta x = 1.0$ mm, $\Delta y = 0.577\,35\Delta x = 0.577\,35$, $\Delta z = 0.5296$ mm, $\Delta t = \Delta z/2C_0$, and Gaussian half-width $= 16$ ps. Microstrip line width was modeled as $7\Delta y$, the reference plane was set at a distance $12\Delta x$ from the source plane.

C. Modeling of Three-Element CMTRA

The application of FDTD method is similar to the application of single rings. The mesh size was considered such that it can model the actual dimensions of the CMTRA. The FDTD parameters were $\Delta x = 0.4$ mm, $\Delta y = 0.230\,94\Delta z = 0.5296$ mm, $\Delta t = \Delta y/2C_0$, and Gaussian half-width $= 20$ ps.

In all three cases Mur's first-order absorbing boundary condition had been applied at the end, side, and top walls [4]. The total and incident E field were stored at the reference plane. Frequency-dependent scattering parameter was

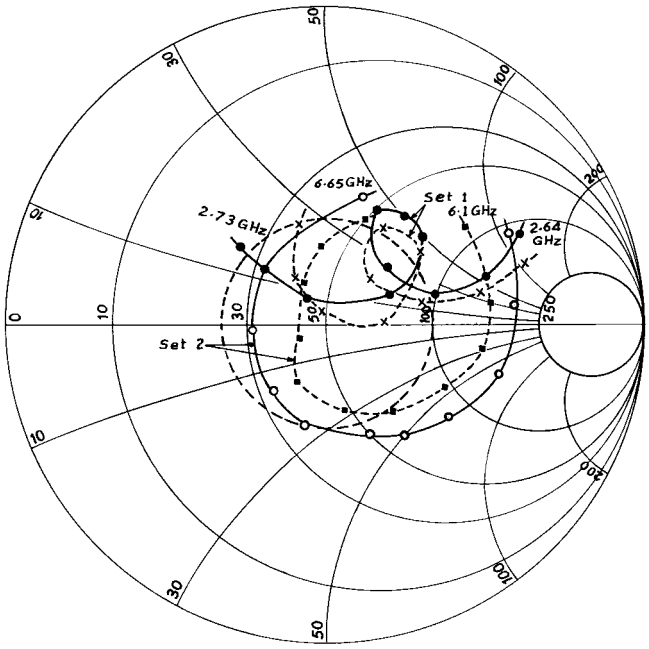

(a)

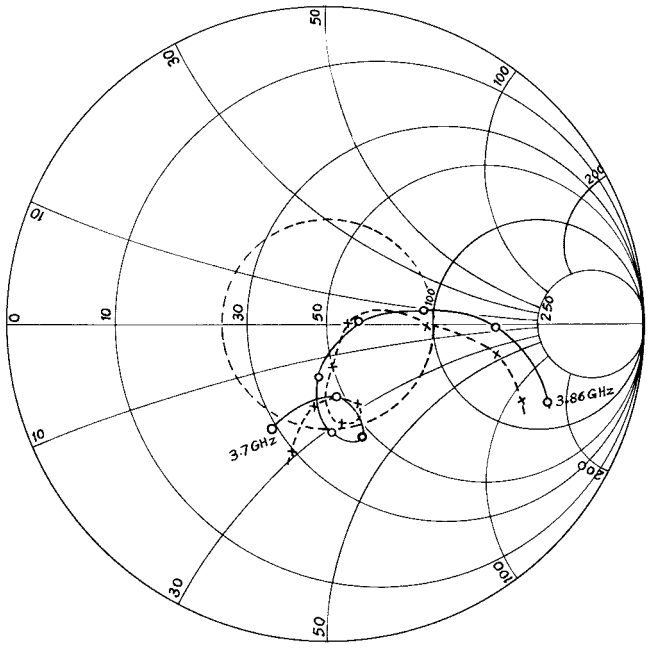

(b)

Fig. 6. (a) and (b) Impedance plot of three-element CMTRA at different frequency band for 0.35-cm off-center feed.

computed following the procedure as described in [1] and [5] and from this input impedance of the antennas were calculated.

IV. Measurements and Results

A. Impedance Pattern

The variation of input impedance for the two STRA and CMTRA were measured by HP 8410B network analyzer at different band of frequencies. For the large single ring and CMTRA impedance patterns are measured at different feed locations to observe the effect of feed location. The impedance patterns for the largest and smallest the single ring antennas are given in Figs. 3 and 4 and for the CMTRA are given in Figs. 5 and 6. The 2:1 VSWR circles are shown in the corresponding figures.

TABLE I
Comparison of 2:1 VSWR %BW of STRA and CMTRA

Antenna	Feed location	Freq. Range in GHz	%BW
Smallest STRA	CF	5.950 - 6.180 = 0.230	3.790
Largest STRA	CF	2.730 - 2.770 = 0.040	*1.4540
	0.35 cm OCF	2.730 - 2.755 = 0.025	0.9110
	0.60 cm OCF	2.725 - 2.735 = 0.010	0.3660
CMTRA	CF	2.730 - 2.790 = 0.060	2.1700
		4.600 - 4.710 = 0.110	2.3630
		6.650 - 6.920 = 0.270	3.9700
	0.35 cm OCF	2.660 - 2.730 = 0.070	**2.5900
		3.700 - 3.830 = 0.130	*3.4520
		6.340 - 6.620 = 0.280	*4.3200
	0.60 cm OCF	2.660 - 2.690 = 0.030	1.1200
		2.720 - 2.745 = 0.025	0.9149
		3.690 - 3.830 = 0.140	3.7200
		6.400 - 6.600 = 0.200	3.0760

CF = Center Feed, OCF = Off Center Feed,
* = 2.2 : 1 VSWR, ** = 2.4 : 1 VSWR

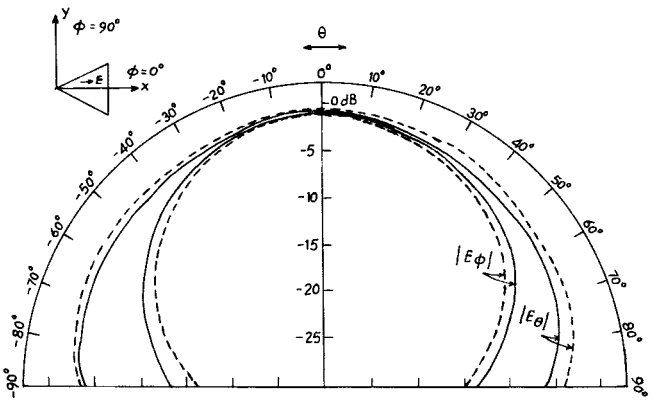

Fig. 7. Measured radiation patterns for largest triangular-ring antenna at different feed locations.

B. Bandwidth

The computed 2:1 VSWR bandwidth for single ring and CMTRA at different band and feed locations are given in Table I. From this table it is seen that increase in bandwidth is obtained for CMTRA as compared to a single ring and maximum total bandwidth is obtained at a feed location 0.35 cm away from center for this particular CMTRA.

C. Radiation Patterns

The radiation patterns for STRA and three-element CMTRA have been measured for both $\varphi = 90°$ and $\varphi = 0°$ planes over the entire bandwidth of the antenna and are plotted in Figs. 7–10. Comparison of the radiation pattern of a single

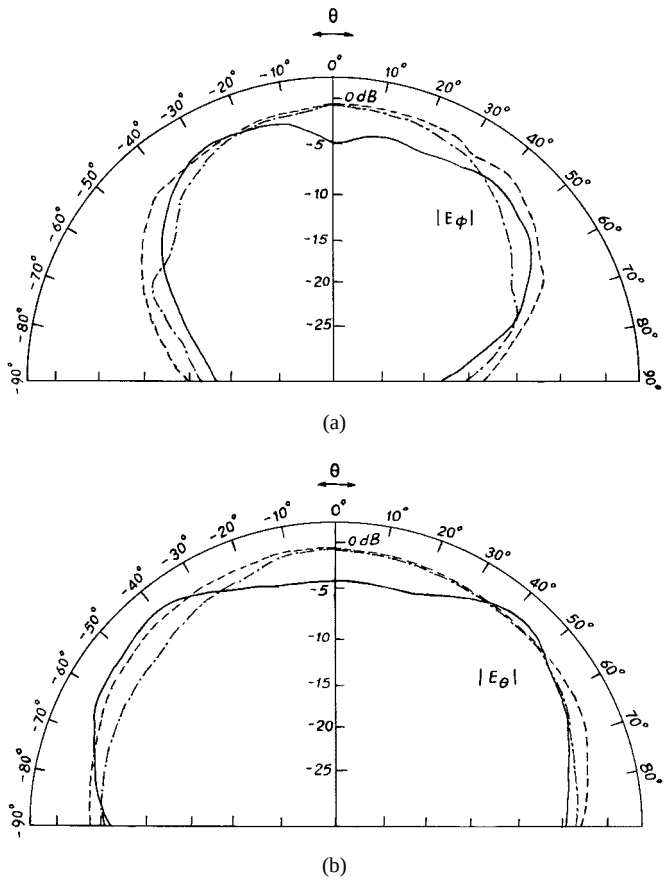

Fig. 8. Measured radiation patterns for three-element CMTRA for center feed (a) at $\varphi = 90^0$ plane and (b) at $\varphi = 0^0$ plane.

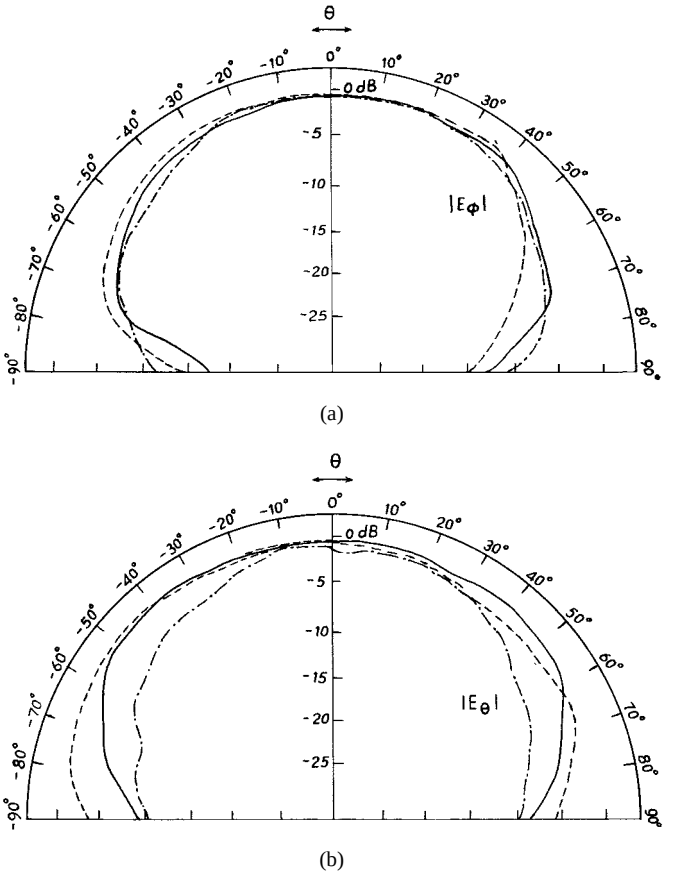

Fig. 9. Measured radiation patterns for three-element CMTRA for 0.35-cm off-center feed (a) at $\varphi = 90^0$ plane and (b) at $\varphi = 0^0$ plane.

ring and CMTRA shows that over the entire bandwidth the nature of the radiation pattern is qualitatively similar to that of the single ring operating at the fundamental mode. Again from Figs. 8–10 it is seen that radiation patterns for CMTRA remain unchanged with the change of feed location.

V. Numerical Results

The FDTD impedance patterns for the single rings and CMTRA are computed for the center feed and for 0.35-cm off-center feed and are plotted in Figs. 3–6 with the measured patterns. From these figures it is seen that the computed patterns are in reasonable agreement with the experimental one. The difference between the computed data and the experimental one may be due to the consideration of original FDTD algorithm for the slanted planes. A simple method of correcting this algorithm is described below [3].

Consider a rectangular cell, located at a metallic boundary that crosses the cell along its diagonal as shown in Fig. 11. The proper FDTD formulation for the fields relevant to the cell is obtained from the integral form of Maxwell's equations

$$\int \mathbf{H}.d\mathbf{l} = \iint_S (\in d\mathbf{E}/dt + \sigma\mathbf{E}).ds \tag{3a}$$

$$\int \mathbf{E}.d\mathbf{l} = \iint_S -(\mu d\mathbf{H}/dt).ds. \tag{3b}$$

Applying (3b) to the cell of Fig. 11, we obtain

$$\begin{aligned} &E_x^n(i+1/2,\, j,\, k)\Delta x + E_y^n(i+1,\, j+1/2,\, k)\Delta y \\ &\quad - E_{\text{slant}}^n(i+1/2,\, j+1/2,\, k)\sqrt{(\Delta x^2+\Delta y^2)} \\ &\quad = -(\mu\Delta x\Delta y/2\Delta t)[H_z^{n+1/2}(i+1/2,\, j+1/2,\, k) \\ &\quad - H_z^{n-1/2}(i+1/2, j+1/2, k)] \end{aligned} \tag{4}$$

where Δx, Δy, Δz are the space steps, Δt is the time steps according to the Yee's [6] formulation. E_{slant} is the E field along the diagonal of the cell and is zero on the metallic wall. From (4) H_z can be easily calculated as follows:

$$\begin{aligned} &H_z^{n+1/2}(i+1/2,\, j+1/2,\, k) \\ &\quad = H_z^{n-1/2}(i+1/2,\, j+1/2,\, k) \\ &\quad - (2\Delta t/\mu\Delta x\Delta y).[E_x^n(i+1/2,\, j,\, k)\Delta x \\ &\quad + E_y^n(i+1,\, j+1/2,\, k)\Delta y]. \end{aligned} \tag{5}$$

The modified (5) for the triangular cell differs from the conventional one only by a factor of two in the right-hand side. This simply corresponds to the cell having half the surface. This technique can be used to conform the mesh to any slanted plane wall by choosing the proper aspect ratio of the cell as described in this paper for the triangular-ring antenna.

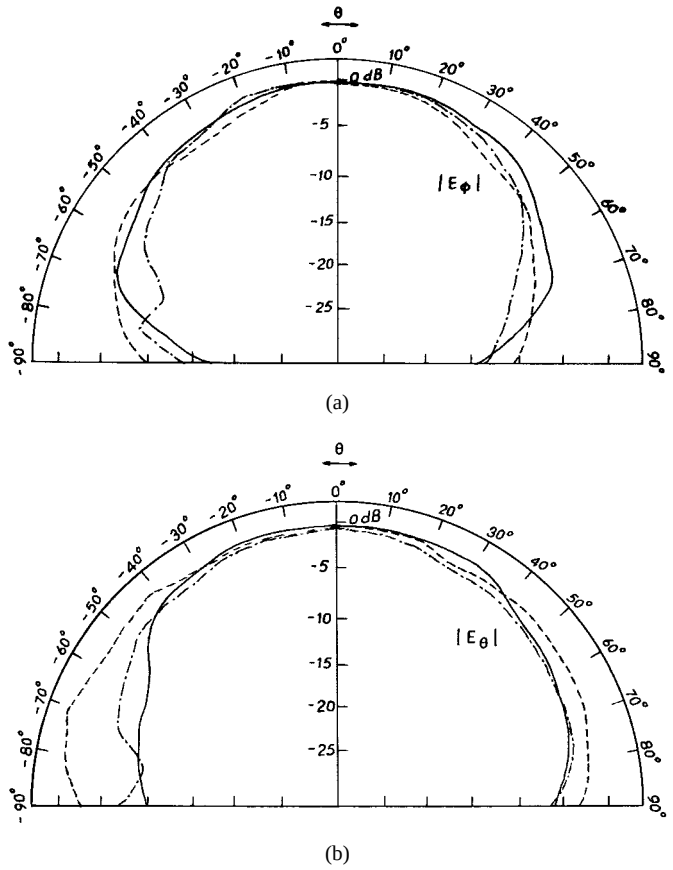

(a)

(b)

Fig. 10. Measured radiation patterns for three-element CMTRA for 0.6-cm off-center feed (a) at $\varphi = 90^0$ plane and (b) at $\varphi = 0^0$ plane.

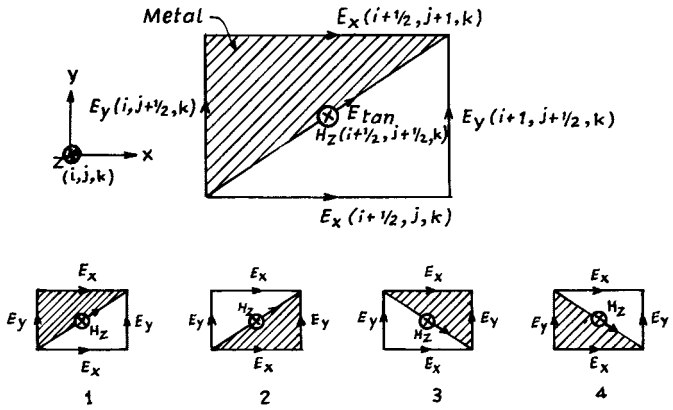

Fig. 11. Enlargement of a cell close to the slanted metallic surface.

Consider the four cases (Fig. 11), which occur in the metallic boundary of the triangular ring as indicated by the line number 1, 2, 3, and 4 in Fig. 2. Applying (5) in these four cases the modified equations for H_z are given by the following:

Case 1:

$$H_z^{n+1/2}(i+1/2,\, j+1/2,\, k) = H_z^{n-1/2}(i+1/2, j+1/2, k) - (2\Delta t/\mu\Delta x\Delta y) * [E_x^n(i+1/2,\, j,\, k)\Delta x + E_y^n(i+1,\, j+1/2,\, k)\Delta y] \quad (6a)$$

Case 2:

$$H_z^{n+1/2}(i+1/2,\, j+1/2,\, k) = H_z^{n-1/2}(i+1/2,\, j+1/2,\, k) - (2\Delta t/\mu\Delta x\Delta y) * [E_x^n(i+1/2,\, j+1,\, k)\Delta x + E_y^n(i,\, j+1/2,\, k)\Delta y] \quad (6b)$$

Case 3:

$$H_z^{n+1/2}(i+1/2,\, j+1/2,\, k) = H_z^{n-1/2}(i+1/2,\, j+1/2,\, k) - (2\Delta t/\mu\Delta x\Delta y) * [E_x^n(i+1/2,\, j,\, k)\Delta x - E_y^n(i,\, j+1/2,\, k)\Delta y] \quad (6c)$$

Case 4:

$$H_z^{n+1/2}(i+1/2,\, j+1/2,\, k) = H_z^{n-1/2}(i+1/2,\, j+1/2,\, k) - (2\Delta t/\mu\Delta x\Delta y) * [E_x^n(i+1/2,\, j+1,\, k)\Delta x - E_y^n(i+1,\, j+1/2,\, k)\Delta y]. \quad (6d)$$

These modified equations for the H_z field have been implemented on the smaller triangular-ring antenna for impedance calculation. The calculated impedance pattern for this antenna is given in Fig. 4 with the measured and general FDTD algorithm patterns and Fig. 4 reveals the accuracy of the new system of equations. This method was applied to CMTRA considered earlier for center feed and the result shows less deviation from the experimental value.

VI. Conclusion

From the above investigations it may be said that the concentric micorstrip triangular ring antenna has a multiple band effect with increase in total % bandwidth with respect to the single ring having the largest and the smallest physical dimension of the CMTRA. Changing the location of the feed the total % bandwidth is increased and with the changed feed location radiation patterns of the CMTRA remain unaltered. Comparison of the experimental impedance patterns with the FDTD patterns shows the validity of the modeling of the triangular-ring structures as described in this paper. The most attractive feature of this structure is the increase of impedance and radiation band width without losing the advantage of small size of microstrip antenna.

Acknowledgment

The authors would like to thank Council of Scientific and Industrial Research (CSIR), India, and Microwave Laboratory of Electronics and Telecom Engineering Department of Jadavpur University, Calcutta, India, for providing resources required for the research.

References

[1] I. S. Misra and S. K. Chowdhury, "Concentric microstrip ring antenna: Theory and experiment," *J. Electromagn. Waves Applicat.*, vol. 10, pp. 439–450, 1996.

[2] J. Fang and J. Ren, "A locally conformed finite-difference time-domain algorithm of modeling arbitrary shape planar metal strips," *IEEE Trans. Microwave Theory Tech.*, vol. 41, pp. 830–838, May 1993.
[3] P. Mezzanette, L. Roselli, and R. Sorrentino, "A simple way to model curved metal boundaries in FDTD algorithm avoiding staircase approximation," *IEEE Microwave Guided Wave Lett.*, vol. 5, pp. 267–269, Aug. 1995.
[4] G. Mur, "Absorbing boundary conditions for the finite difference approximation of the time domain electromagnetic equations," *IEEE Trans. Electromagn. Compat.*, vol. EMC-2, pp. 377–382, Apr. 1981.
[5] D. M. Sheen, S. M. Ali, M. D. Abouzahra, and J. A. Kong, "Application of the three-dimensional finite difference time-domain method to the analysis of planar microstrip circuits," *IEEE Trans. Microwave Theory Tech.*, vol. 38, pp. 849–857, July 1990.
[6] K. S. Yee, "Numerical solution of initial boundary value problems involving Maxwell's equations in isotropic media," *IEEE Trans. Antennas Propagat.*, vol. AP-14, pp. 302–307, Apr. 1966.

Iti Saha Misra was born in India on September 25, 1964. She received the B.Sc. (Hons.) degree in physics, in 1986, the B.Tech degree in radio physics and electronics, in 1989, from the Calcutta University, India, and the M.E. and Ph.D. degrees in electronics and telecommunications engineering, in 1991 and 1997, respectively, from the Jadavpur University, India.

She is now a Lecturer in the Electronics and Telecommunications Engineering Department at the Jadavpur University. Her research interests are in the areas of electromagnetics in general and microstrip antennas in particular.

S. K. Chowdhury (M'79–SM'83) received the B.Tel.E., M.E.Tel.E., and Ph.D. (engineering) degrees from Jadavpur University, India, in 1964, 1968, and 1972, respectively.

He joined the Department of Electronics and Telecommunication Engineering of Jadavpur University in 1969 as a Lecturer. He is now a Professor in the same department. He has written approximately 50 papers for national and international journals. His current interests include engineering education, electromagnetics, and microwaves, in general, and microstrip antennas and components, in particular.

Dr. Chowdhury is a Fellow IE (India).